Journal of Power Sources 253 (2014) 412–418

Contents lists available at ScienceDirect

Journal of Power Sources

journal homepage: www.elsevier.com/locate/jpowsour

Development of a voltage relaxation model for rapid open-circuit voltage prediction in lithium-ion batteries

Lei Pei*, Tiansi Wang, Rengui Lu, Chunbo Zhu

School of Electrical Engineering and Automation, Harbin Institute of Technology, Harbin 150001, PR China

HIGHLIGHTS

- Discover that diffusion time constant is a linear function of open-circuit time.
- Established a new voltage relaxation model with good curve-fitting performance.
- Presented a rapid, adaptive and online OCV prediction method.
- Shorten the waiting time from traditional 20 h to 20 min with the new method.

ARTICLE INFO

Article history:
Received 5 October 2013
Received in revised form
27 November 2013
Accepted 18 December 2013
Available online 27 December 2013

Keywords:
Lithium-ion battery
Open-circuit voltage
Relaxation model
Time constant
Rapid prediction

ABSTRACT

The open-circuit voltage (OCV) of a battery, as a crucial characteristic parameter, is widely used in many aspects of battery technology, such as electrode material mechanism analysis, battery performance/state estimation and working process management. However, the applications of OCV are severely limited due to the need for a long rest time for full relaxation. In this paper, a rapid OCV prediction method is proposed to predict the final static OCV in a few minutes using linear regression techniques, based on a new mathematical model developed from an improvement on a second-order resistance–capacitance (RC) model. As the improvement, an important discovery is demonstrated by experimental investigation and data analysis: the relaxation time (i.e., time constant) of the diffusion circuit of the second-order RC model is not a fixed constant, unlike an intrinsic value for a given material, but an apparent linear function of the open-circuit time. This improvement enables the new model to track the actual relaxation process very well. The accuracy and the rapidity of the new model and proposed method are validated with working-condition experimental data on battery cells with different cathodes, and the results of OCV prediction are very accurate (errors below 1 mV in 20 min).

1. Introduction

Rechargeable batteries play a significant role in powering many portable applications that have high electric power requirements. For electric vehicles (EVs) (including battery electric vehicles, hybrid electric vehicles and plug-in hybrid electric vehicles) and mobile electronics (such as mobile phones and laptops), the use of a lithium-ion battery as a storage system is currently the best choice based on comprehensive consideration of its energy and power density and cycle-life [1].

The open-circuit voltage (OCV) of the lithium-ion battery, a crucial characteristic parameter, reflects the battery's inertial status and plays an important role in many aspects of battery technology, such as electrode material mechanism analysis, battery performance/state estimation and working process management [2–9]. Because lithium-ion battery OCV depends on the electrode material and the amount of lithium intercalation in it [2,3], the battery OCV can not only be used to analyze the relative electron energies of the electrode materials but can also be used to estimate the state-of-charge (SOC) of the batteries, which indicates the available capacity of the cells [4–6]. The OCV can also be used to estimate the batteries' state-of-health (SOH) because the battery OCV decay occurs only in the high-SOC range during the battery aging process [7]. Additionally, the OCV is used as an important judge basis for cell balancing strategy technology [8,9]. Thus, an accurate determination of the OCV is requested to enable management of the battery in its optimal state.

The battery voltage only equals the static OCV when the battery is under open-circuit conditions and the voltage has been relaxed to its equilibrium. During the rest period, the impacts of the

* Corresponding author. Tel./fax: +86 451 86413621x809.
E-mail address: lei.pei@hotmail.com (L. Pei).

0378-7753/$ – see front matter © 2013 Elsevier B.V. All rights reserved.
http://dx.doi.org/10.1016/j.jpowsour.2013.12.083

measurement current and the side-reaction can be neglected, but a long rest time is always needed (e.g., 20 h). Unfortunately, the long waiting time severely limits the application of the OCV, especially for online working conditions. To overcome this shortcoming of the conventional rest method for the OCV, some studies have been performed to shorten the time for obtaining the OCV in equilibrium [5,6,8,10–12]. A few straightforward methods are presented for lead-acid batteries in earlier papers, e.g., the asymptotes method [10] and the dV/dt method [11]. However, as limited by the use of fixed parameters, these techniques are not appropriate for various working conditions such as different temperatures and SOCs. For lithium-ion cells, a few methods are proposed to predict the final OCV based on the battery voltage and the time measurements of the first several minutes of the relaxation process. In these methods, for simulating the voltage relaxation process, a few mathematical models are presented, including empirical models and equivalent circuit models. In Refs. [5,6], two empirical models are proposed by curve fitting. However, both of them lack a reasonable physical interpretation and the corresponding OCV prediction methods do not always have a reasonable computational effort for an online application. As for a more reasonable physical interpretation, a conventional second-order resistance–capacitance (RC) model with a fixed time constant is used in Ref. [8], but this model does not fit the measured relaxation curve well enough. Additionally, based on a modified second-order RC model, a rapid test-procedure method to derive the OCV is described in Ref. [12]. However, when the method is used in an online application, a few millivolts error of the OCV prediction probably occurs, because the diffusion overpotential of the proposed model is taken as a constant value.

This work aims at developing an accurate and reasonable voltage relaxation model and a low-complexity OCV prediction method. Depending on the study of the relaxation process of the diffusion overpotential, which is caused by the insufficient transport of the reactants and dominates during most of the time of the entire relaxation process, the voltage relaxation model is developed from experimental investigation of the relationship between the open-circuit time and the relaxation time (i.e., the time constant) of the diffusion RC circuit in the second-order RC model. Based on the new model, the rapid, adaptive and online OCV prediction method is proposed, which ensures that the cell OCV can be predicted quickly and accurately under open-circuit conditions with a low computational complexity. Additionally, the accuracy and universality of the new model and the new OCV prediction method are verified on cells with different cathodes.

2. Experiment design

In this research, 32650-type $LiFePO_4$/graphite cells with a capacity of 5 Ah and 32650-type $LiMn_2O_4$/graphite cells with a capacity of 6 Ah were chosen as the research objects. The tests were performed on single cells and divided into two parts. The first part of the tests aims to examine the cell's OCV behavior of relaxation to develop a new relaxation model. The goal of the second part of the tests is to validate the effects of the new model and the new rapid algorithm.

2.1. Relaxation characteristic test

In this part, in order to study the voltage relaxation behaviors after different working conditions and develop a general voltage relaxation model, six tests from (a) to (f) were performed sequentially with different SOC points, temperatures and charge–discharge schedules. Each test can be divided into two steps: the load step and the relaxation step. During the first step (i.e., load step), the cell works according to one of the six set modes detailed in Table 1. During the second step (i.e., relaxation step), the cell was at rest for 20 h to obtain the static OCV that is taken as a true value. If two neighboring tests have the different working temperatures, another 20 h rest period, at the temperature of the latter test, was needed. Additionally, before the tests, the cell was fully charged to SOC = 1 with constant current–constant voltage (CCCV) (a constant current 0.5 C charge until the voltage reaches the upper limit, followed by a constant voltage charge until the current is below 0.05 C). The experiments of this part were only performed on the $LiFePO_4$ cell.

2.2. Validation test

The test in this part was administered to validate the efficacy of the new model and the rapid OCV algorithm. First, the cell was fully charged by CCCV and then rested for 5 h. Second, the federal urban driving schedule (FUDS) test was administered for 1 h. Finally, following a rest of 20 h, the cell voltage was measured as a true value for OCV. To verify the universality of the rapid OCV prediction algorithm, the validation tests were performed on both the $LiFePO_4$ and $LiMn_2O_4$ cells.

2.3. Measurement equipment

All tests were performed with a channel of the Arbin instruments' BT2000 test bench (18 V, ±100 A), which has a voltage measurement accuracy of ±0.01% and a current measurement accuracy of ±0.02% on the full-scale value. An Agilent 34410A 6½-digit multimeter was used as an auxiliary to measure the voltage; the measurement accuracy of the multimeter is less than 0.1 mV for the cell's voltage. Moreover, the cell ambient temperatures were controlled within ±2 °C by incubators in all tests.

3. Proposed model and method

In this section, the battery relaxation behavior will be studied first. Based on the study, a new relaxation model and the corresponding application method will be discussed.

3.1. Results of the characteristic test

Referring to Section 2.1, corresponding to six characteristic tests from (a) to (f), the curves of the load steps are shown in Fig. 1, and the relaxation processes are shown in Fig. 2. When the battery switches from working to open-circuit state, the cell's actual voltage does not immediately reach the equilibrium state because its internal chemical and mechanical processes do not disappear immediately with the current cutoff. The voltage without full relaxation cannot represent the cell's OCV that coincides with the battery's electro-motive force (EMF) [13]. Herein, the EMF is the voltage measured across the anode and cathode, and equals the

Table 1
The details for the load steps of the characteristic tests from (a) to (f). Herein, the SOCs are measured by a coulomb counting method.

Test	Temperature	Charge–discharge process
(a)	30 °C	Discharge from SOC = 1 to SOC = 0.9 with 2 C
(b)	30 °C	Federal urban driving schedule (FUDS) cycle test from SOC = 0.9 to SOC = 0.7
(c)	50 °C	Discharge from SOC = 0.7 to SOC = 0.4 with 0.5 C
(d)	10 °C	Discharge from SOC = 0.4 to SOC = 0.3 with 0.5 C
(e)	30 °C	Charge from SOC = 0.3 to SOC = 0.5 with 1 C
(f)	30 °C	Charge from SOC = 0.5 to SOC = 0.8 with 0.5 C

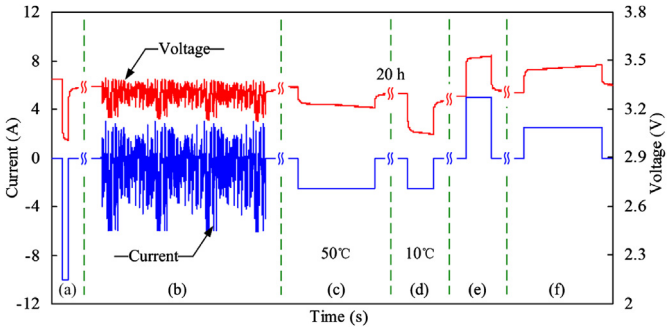

Fig. 1. The profiles of the various load processes in the characteristic tests from (a) to (f).

difference of the lithium chemical potentials between the two electrodes [3]. Although the remnant overpotential will degrade along with the relaxation process, this process still takes a long time (e.g., 20 h).

By comparing the six relaxation curves in Fig. 2, distinct differences in the relaxation behavior can be found in the aspects of the value or shape, which means that when the battery is in nonequilibrium, it is almost impossible to shorten the time to obtain the static OCV by removing a fixed deviation from the measured voltage at a fixed time and it is also almost impossible to calculate static OCV from a fixed-parameter relaxation model.

To be able to online predict the final static OCV in a short time, two requirements need to be met: first, a model, that can accurately fit the actual relaxation behavior needs to be developed, and second, a training-free method to online identify the model's parameters including the OCV is needed to support the application of the developed model with reasonable computational complexity.

3.2. Relaxation model

Generally, a second-order RC model is always used to describe the dynamic and static characteristic of the battery [8,13–16]. As shown in Fig. 3, this model is mainly composed of three parts including the OCV, the ohmic resistance (R_o) and the polarization part, which consists of two RC-equivalent circuits to separately simulate the characteristics of the activation polarization and the concentration polarization in the battery.

Based on this model, the battery voltage (U_{bat}) can be represented as Eq. (1). In this equation, the ohmic overpotential (η_o) corresponds to voltage drop on the ohmic resistance, and the

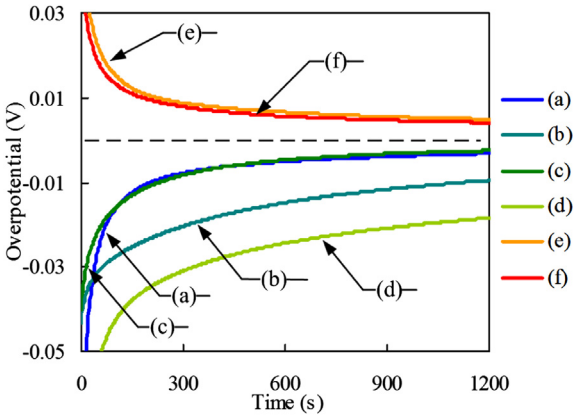

Fig. 2. The contrast of the relaxation processes after various load conditions.

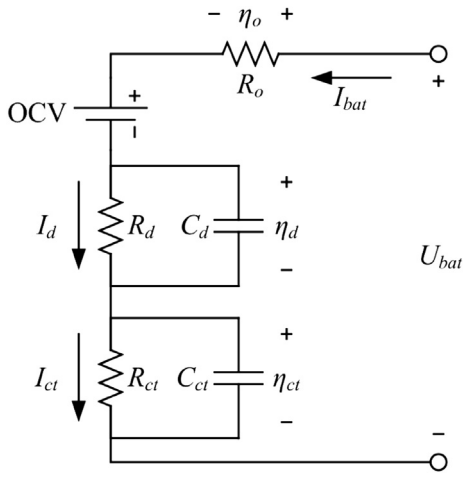

Fig. 3. The second-order RC circuit model.

charge transfer overpotential (η_{ct}) and the diffusion overpotential (η_d) are caused by the activation polarization and the concentration polarization separately. As soon as the circuit is opened (i.e., the load current I_{bat} equals zero), the η_o will immediately disappear, but the η_{ct} and η_d will gradually decay until the battery has fully relaxed [17]. Thus, during the battery relaxation process, the OCV, η_{ct} and η_d are collectively referred to as a relaxation voltage (U_{RLX}).

$$U_{bat} = \underbrace{\mathrm{OCV} + \eta_d + \eta_{ct}}_{U_{RLX}} + \eta_o \tag{1}$$

In the model, according to the different polarization mechanisms, the time of full relaxation for the charge transfer process (activation polarization) and the diffusion process (concentration polarization) are apparently different. The charge transfer process proceeds relatively quickly, during which the actual chemical reaction takes place at the interface between the electrode and the electrolyte. In contrast, the diffusion (i.e., mass transport) process is a relatively slow process, in which the materials transformed in the charge transfer process move on from the electrode surface to the interior. This process does not finish until all the materials have been transported [17,18]. Specifically, the time of full relaxation for η_{ct} (i.e., T_{ct}) is always less than 1 min, but the one for η_d (i.e., T_d) is always more than several hours [12,18,19]. Based on the above analysis, Eq. (1) can be rewritten as the discrete-time and segmented form shown in Eq. (2), where $U_{RLX,k}$, $\eta_{ct,k}$ and $\eta_{d,k}$ denote the corresponding values at the open-circuit moments of t_k.

$$U_{RLX,k} = \begin{cases} \mathrm{OCV} + \eta_{d,k} + \eta_{ct,k}, & 0 < t_k \le T_{ct}, \\ \mathrm{OCV} + \eta_{d,k}, & T_{ct} < t_k \le T_d, \\ \mathrm{OCV}, & T_d < t_k. \end{cases} \tag{2}$$

In Eq. (2), the second function is the main bottleneck limiting the OCV application because the process, during which the η_{ct} has fully relaxed but the η_d still exists, accounts for most of the time of the entire relaxation process. In other words, the manner in which the behavior of the diffusion process is modeled is the key factor in shortening the time for the OCV prediction.

In the traditional second-order RC model, the relaxation time (i.e., the time constant) of the diffusion RC circuit (i.e., τ_d) does not change with the open-circuit time. However, the RC circuit with the fixed time constant cannot fit the actual curve well enough, as shown in Fig. 4. In this figure, two typical curves, which correspond

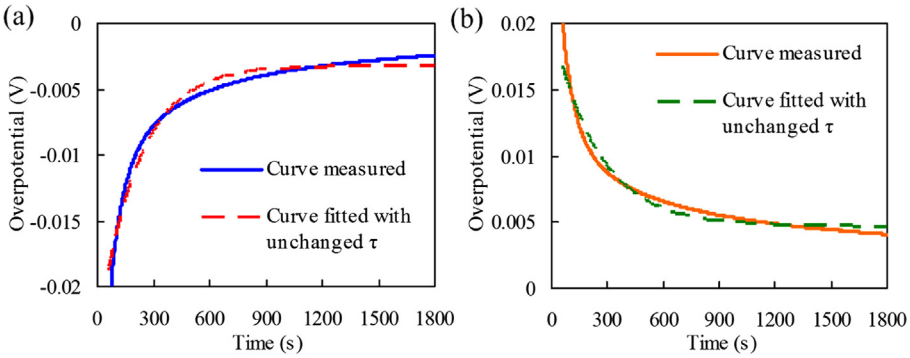

Fig. 4. The fitting curves of the traditional second-order RC model: (a) corresponding to Test (a) in Section 2.1; (b) corresponding to Test (e) in Section 2.1.

to curves (a) and (e) of Fig. 2, are chosen to represent the relaxation process after a charge process or a discharge process, and each curve is best fitted by the RC circuit in the least-squares sense. As can be found by comparing the measured and fitted curves, as the open-circuit time increased, the relaxation rate of the RC circuits leads the rate of the actual curves by a greater extent, which means that the τ_d will not be a constant but instead continues to increase with increasing open-circuit time. Thus, a time-varying τ_d should be used in this study.

To obtain the relationship between the τ_d and the open-circuit time, the values of τ_d at different time points need to be obtained first. In the RC circuit, the discrete recursive formula of the voltage can be expressed as Eq. (3). Taking the transform of Eq. (3), the τ_d at different time points can be obtained from Eq. (4).

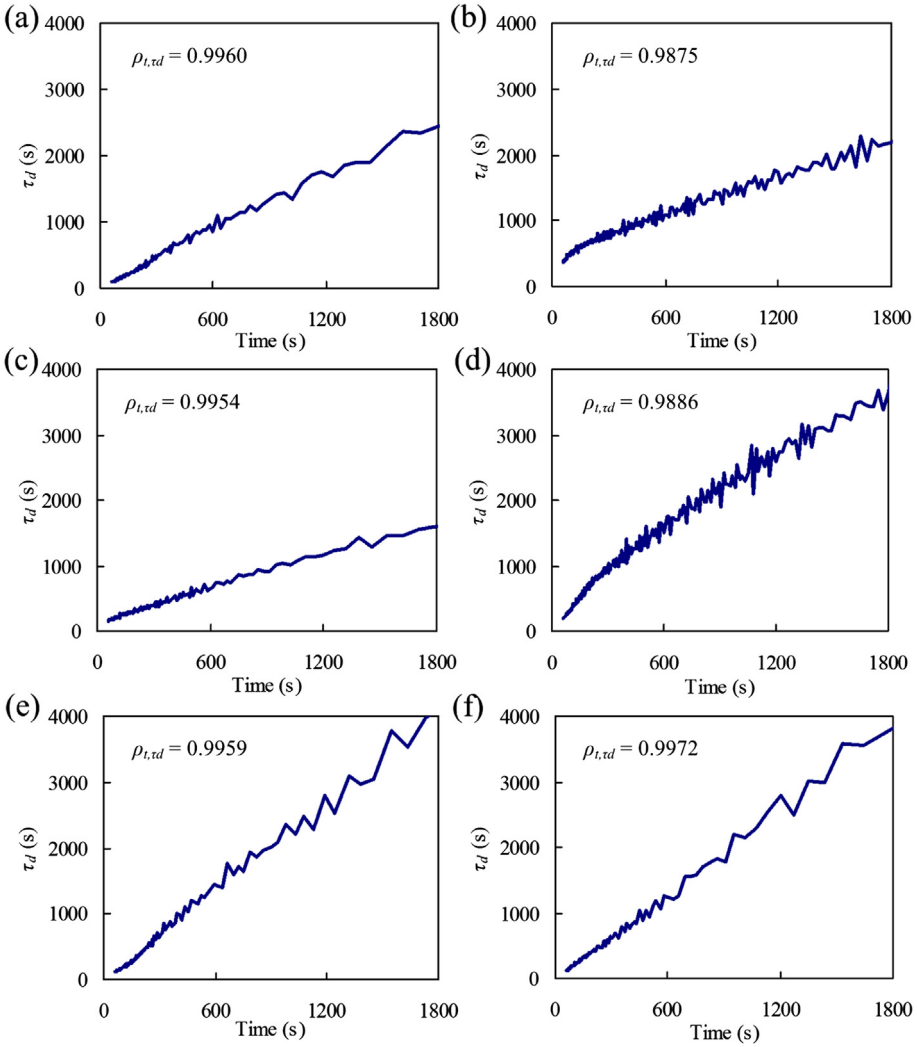

Fig. 5. The relationship between the diffusion relaxation time and the open-circuit time.

$$\eta_{d,k} = \eta_{d,k-1} \times \exp\left[\frac{-(t_k - t_{k-1})}{\tau_{d,k}}\right] \quad (3)$$

$$\tau_{d,k} = \frac{t_k - t_{k-1}}{\ln|U_{RLX,k-1} - \mathrm{OCV}| - \ln|U_{RLX,k} - \mathrm{OCV}|}, \quad t_k > T_{ct} \quad (4)$$

Applying the data from the six tests to Eq. (4), with T_{ct} equal to 1 min, the τ_d curves plotted against open-circuit time are shown in Fig. 5 τ_d will increase with the open-circuit time, as in the above analysis, and there is an obvious linear relationship between the values, as shown in Fig. 5. In the six cases, the correlation coefficients between τ_d and open-circuit time are (a) 0.9960, (b) 0.9875, (c) 0.9954, (d) 0.9886, (e) 0.9959, and (f) 0.9972. Differing from a fixed value of the τ_d for a given material with a known geometry, this non-intrinsic but apparent linear relationship is most likely caused by the use of composite electrodes in commercial full cells.

Based on the linear relationship obtained, a new diffusion overpotential relaxation model is presented. In the new model, the τ_d is a linear function of the open-circuit time, as in Eq. (5), in which α and β will be determined online. Applying Eq. (5) to Eq. (3), the new diffusion overpotential relaxation model's discrete recursive formula can be written as Eq. (6). Then, the battery voltage relaxation model can be written as Eq. (7) during the diffusion relaxation process, where the OCV, α and β are the parameters that need to be fitted online.

$$\tau_{d,k} = \alpha t_k + \beta \quad (5)$$

$$\eta_{d,k} = \eta_{d,k-1} \times \exp\left[\frac{-(t_k - t_{k-1})}{\alpha t_k + \beta}\right] \quad (6)$$

$$U_{RLX,k} = U_{RLX,k-1} \times \exp\left[\frac{-(t_k - t_{k-1})}{\alpha t_k + \beta}\right] - \mathrm{OCV} \times \exp\left[\frac{-(t_k - t_{k-1})}{\alpha t_k + \beta}\right] + \mathrm{OCV}, \; t_k > T_{ct} \quad (7)$$

3.3. Rapid OCV prediction method

Based on the new voltage relaxation model, the OCV and the other model parameters, including α and β, can be found by best fitting the new relaxation model to all the sample gained points (t_k, $U_{RLX,k}$) in the least-squares sense. However, due to the high nonlinearity of the new equations, which results in high computational complexity of the fitting, the prediction process must rely on professional data fitting tools, so it cannot run in online workplaces, such as EVs or mobile electronics.

To reduce the computational complexity and obtain the best solution of the unknown values of the OCV, α and β, the solving process is linearized as below. In the RC circuit, τ_d can be written as Eq. (8a), where R_d is diffusion resistance and C_d is diffusion capacitor in the diffusion circuit. If C_d is formed in the differential expression, Eq. (8a) can be rewritten as Eq. (8b), where ΔQ_d is the charge variation of C_d between two neighboring sampling points and I_d is the current that flows through R_d. The application of the linear relationship between τ_d and open-circuit time (i.e., Eq. (5)) into Eq. (8b) yields Eq. (9). By rearranging Eq. (9), a linear expression about the unknown vector $[\mathrm{OCV}\ \alpha\ \beta]^{\mathrm{T}}$ can be formed, as shown in Eq. (10), where X_k and Y_k are calculated by the sample gained points (t_k, $U_{RLX,k}$) and $M = [\mathrm{OCV}\ \alpha\ \beta]^{\mathrm{T}}$ is the target vector to be determined.

$$\tau_{d,k} = R_{d,k} C_{d,k} \quad (8a)$$

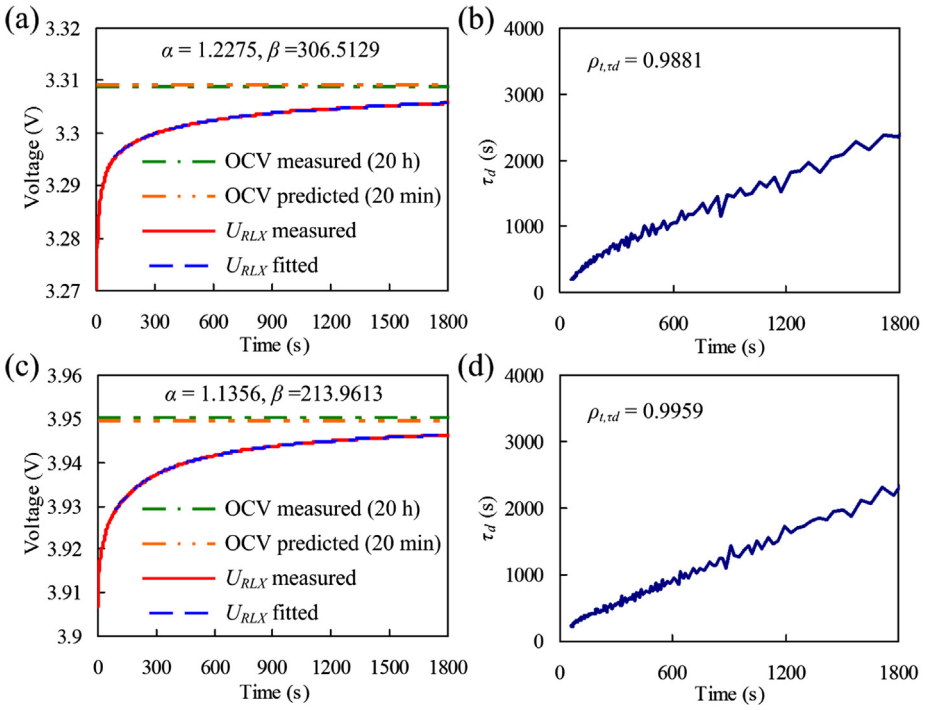

Fig. 6. Validation test: (a) the results of OCV prediction and voltage relaxation curve fitting for the $LiFePO_4$ battery; (b) the linear relationship for the $LiFePO_4$ battery; (c) the results of OCV prediction and voltage relaxation curve fitting for the $LiMn_2O_4$ battery; (d) the linear relationship for the $LiMn_2O_4$ battery.

$$\tau_{d,k} = \frac{R_{d,k}\Delta Q_{d,k}}{\Delta\eta_{d,k}} = \frac{-R_{d,k}(I_{d,k}+I_{d,k-1})(t_k-t_{k-1})}{2(\eta_{d,k}-\eta_{d,k-1})} = \frac{-(\eta_{d,k}+\eta_{d,k-1})(t_k-t_{k-1})}{2(\eta_{d,k}-\eta_{d,k-1})} \quad (8b)$$

$$\alpha t_k + \beta = \frac{-(U_{RLX,k}+U_{RLX,k-1}-2\times\mathrm{OCV})(t_k-t_{k-1})}{2(U_{RLX,k}-U_{RLX,k-1})}, \quad t_k > T_{ct} \quad (9)$$

To determine the target vector, a linear overdetermined system is constructed with a series of linear equations (i.e., Eq. (10) of different sample time points), as in Eq. (11a), where the expressions of X and Y can be found in Eq. (11b). Solving the overdetermined linear equations using Eq. (12) yields the best solution for the target vector including the OCV, which is the best prediction value based on the new relaxation model.

$$Y = XM \quad (11a)$$

$$\underbrace{\frac{(U_{RLX,k}+U_{RLX,k-1})(t_k-t_{k-1})}{2}}_{Y_k} = \underbrace{\begin{bmatrix} (t_k-t_{k-1}) \\ -t_k(U_{RLX,k}-U_{RLX,k-1}) \\ -(U_{RLX,k}-U_{RLX,k-1}) \end{bmatrix}^{\mathrm{T}}}_{X_k} \underbrace{\begin{bmatrix} \mathrm{OCV} \\ \alpha \\ \beta \end{bmatrix}}_{M}, \quad t_k > T_{ct} \quad (10)$$

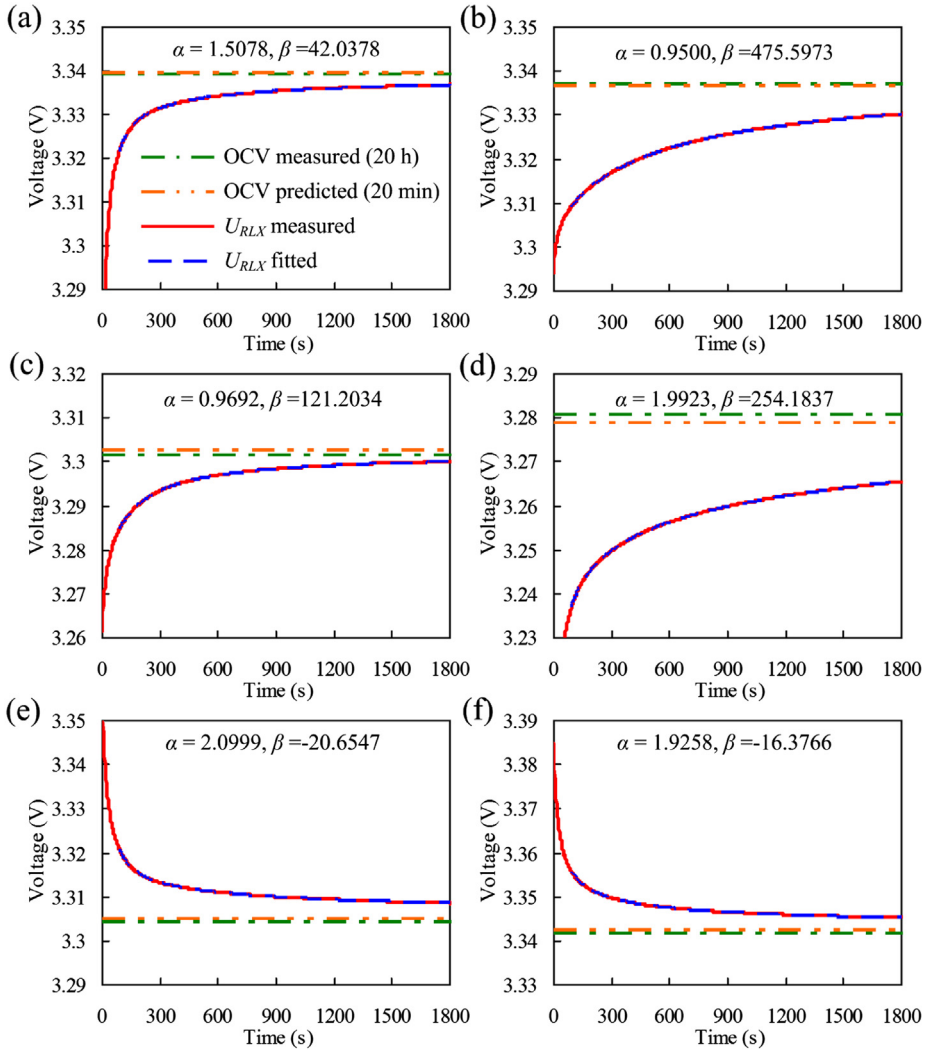

Fig. 7. The results of OCV prediction and voltage relaxation curve fitting for the relaxation characteristic tests.

$$\begin{cases} M = \begin{bmatrix} \mathrm{OCV} \\ \alpha \\ \beta \end{bmatrix} \\ X = \begin{bmatrix} (t_1 - t_0) & -t_1(U_{RLX,1} - U_{RLX,0}) & -(U_{RLX,1} - U_{RLX,0}) \\ \vdots & \vdots & \vdots \\ (t_k - t_{k-1}) & -t_k(U_{RLX,k} - U_{RLX,k-1}) & -(U_{RLX,k} - U_{RLX,k-1}) \end{bmatrix} \\ Y = \begin{bmatrix} (U_{RLX,1} + U_{RLX,0})(t_1 - t_0)/2 \\ \vdots \\ (U_{RLX,k} + U_{RLX,k-1})(t_k - t_{k-1})/2 \end{bmatrix} \end{cases} \tag{11b}$$

$$M = \left[X^{\mathrm{T}}X\right]^{-1}X^{\mathrm{T}}Y \tag{12}$$

In this method, more sampling data will yield more information for solving the unknown vector while simultaneously increasing the waiting time. With comprehensive consideration of the accuracy and rapidity of the method, an open-circuit time of 10–30 min is recommended on the basis of many previous experiments.

4. Validating results

Applying the new model and the corresponding OCV prediction method to the data collected from the validation experiments performed on both $LiFePO_4$ and $LiMn_2O_4$ cells in Section 2.2. The results of the validations are shown in Fig. 6. Wherein, Fig. 6(a) and (c) show the battery voltage values during the relaxation processes and the final OCVs measured after a rest of 20 h for $LiFePO_4$ and $LiMn_2O_4$ cells, respectively. The fitting curves of the new model and the predicted OCVs (and the corresponding values of α and β) based on the first 20 min of data (with a sampling period of 2 s) can also be found in the same figures. As observed from the figures, the new model fits the actual relaxation process very well, and the prediction error is less than 1 mV (−0.5 mV for $LiFePO_4$ and 0.7 mV for $LiMn_2O_4$), indicative of method universality. Additionally, the τ_d curves plotted against time for $LiFePO_4$ and $LiMn_2O_4$ cells are presented in Fig. 6(b) and (d), respectively, which both reflect a good linear relationship with correlation coefficients of 0.9881 and 0.9959, respectively.

Moreover, the proposed OCV prediction method is implemented on the six cases corresponding to the relaxation characteristic tests (a) to (f) referred to in Section 2.1, respectively, and the results, based on the first 20 min of data, are shown in the subfigures from (a) to (f) of Fig. 7, which also show good curve-fitting effects and accurate prediction results with errors of (a) 0.3 mV, (b) −0.7 mV, (c) 0.9 mV, (d) −1.7 mV, (e) 0.6 mV, and (f) 0.5 mV. In contrast, the prediction results of the traditional second-order RC model are much worse, with errors of (a) −3.9 mV, (b) −8.2 mV, (c) −2.8 mV, (d) −18.6 mV, (e) 5.5 mV, and (f) 4.5 mV based on the same data.

There can be found only small errors ($\leq$1 mV) of the OCV values predicted in a short time except for the value (−1.7 mV) at 10 °C, suggesting a good robustness of the new model and the proposed method. The larger error occurs, probably because at a lower temperature, battery parameters are more sensitive to the inhomogeneity of the inner battery temperature caused by the internal heat generated on-load due to the internal resistance.

5. Conclusions

In this paper, a linear relationship between the diffusion relaxation time (i.e., the diffusion time constant) of the second-order RC model and the open-circuit time was discovered based on the experimental investigation of the OCV relaxation behaviors for lithium-ion batteries. This discovery will probably replace the traditional constant relaxation time and become popular in future research in related fields. Based on the linear relationship, a new voltage relaxation model was presented, which can fit and simulate the battery dynamic relaxation process very well.

Furthermore, a linear regression method was provided for the new model to rapidly predict the static OCV, which can shorten the traditional rest time and reduce the computational complexity. With this method, the model parameters will be identified online on the basis of the battery voltage and time measurements; thus, the overall concept can be used for other electrode materials or under different working conditions. In the validation experiments, the presented OCV prediction method shows satisfactory results with rapidity (20 min instead of 20 h) and accuracy (errors $\leq$ 1 mV except at a lower temperature) and indicates good universality for two types of lithium-ion batteries.

The effects of low temperature on the OCV relaxation process will be further studied in the future work.

Acknowledgments

This research was supported by the National High Technology Research and Development Program of China (2012AA111003) in part and the International (Regional) Cooperation and Exchange between the National Natural Science Funds of China and the UK Engineering and Physical Sciences Research Council (51361130153) in part. The author would also like to thank the reviewers for their corrections and helpful suggestions.

References

[1] B. Scrosati, J. Garche, J. Power Sources 195 (2010) 2419–2430.
[2] J.B. Goodenough, Y. Kim, Chem. Mater. 22 (2010) 587–603.
[3] A. Van der Ven, J. Bhattacharya, A.A. Belak, Acc. Chem. Res. 46 (2012) 1216–1225.
[4] S. Piller, M. Perrin, A. Jossen, J. Power Sources 96 (2001) 113–120.
[5] V. Pop, H.J. Bergveld, D. Danilov, P.P.L. Regtien, P.H.L. Notten, Methods for Measuring and Modelling a Battery's Electro-motive Force, Springer, Netherlands, 2008, pp. 63–94.
[6] L. Pei, R. Lu, C. Zhu, IET Electr. Syst. Transp. 3 (2013) 112–117.
[7] M.A. Roscher, J. Assfalg, O.S. Bohlen, IEEE Trans. Veh. Technol. 60 (2011) 98–103.
[8] P.A. Cassani, S.S. Williamson, IEEE Trans. Ind. Electron. 57 (2010) 3956–3962.
[9] W.L. Chen, J.F. Li, B.X. Huang, Electr. Power Compon. Syst. 39 (2011) 1632–1646.
[10] J.H. Aylor, A. Thieme, B.W. Johnso, IEEE Trans. Ind. Electron. 39 (1992) 398–409.
[11] S. Hoenig, H. Singh, T.G. Palanisamy, US Patent 6,366,054, 2001.
[12] S. Abu-Sharkh, D. Doerffel, J. Power Sources 130 (2004) 266–274.
[13] H.J. Bergveld, Battery Management Systems: Design by Modelling, Enschede, 2001.
[14] J. Remmlinger, M. Buchholz, M. Meiler, P. Bernreuter, K. Dietmayer, J. Power Sources 196 (2011) 5357–5363.
[15] Z. Chen, C.C. Mi, Y. Fu, J. Xu, X. Gong, J. Power Sources 240 (2013) 184–192.
[16] S. Sepasi, R. Ghorbani, B.Y. Liaw, J. Power Sources 245 (2014) 337–344.
[17] M. Park, X. Zhang, M. Chung, G.B. Less, A.M. Sastry, J. Power Sources 195 (2010) 7904–7929.
[18] E. Ofek, WIPO Patent Application WO/2009/128,079, 2009.
[19] C.L. Schmidt, P.M. Skarstad, J. Power Sources 65 (1997) 121–128.